Induced Fit and Mobility of Cycloalkanes within Nanometer-sized Confinements at 5K

Aisha Ahsan[a*], Luiza Buimaga-Iarinca[b], Thomas Nijs[a], Sylwia Nowakowska[a], Rejaul Sk[a], S. Fatemeh Mousavi[a], Mehdi Heydari[c], Meike Stöhr[d], Sameena S. Zaman[e], Cristian Morari[b], Lutz H. Gade[f*], Thomas A. Jung[c*]

[a]Dr. A. Ahsan, Dr. S. F. Mousavi, Dr. T. Nijs, Dr. S. Nowakowska, Dr. Rejaul Sk

Department of Physics, University of Basel, Klingelbergstrasse 82, 4056 Basel, Switzerland, E-mail: aisha.ahsan@unibas.ch

[b]Dr. L.Buimaga- Iarinca, Dr. C. Morari

CETATEA, National Institute for Research and Development of Isotopic and Molecular Technologies, 67-103 Donat, 400293 Cluj-Napoca, Romania, E-mail: luiza.iarinca@itim-cj.ro; cristian.morari@itim-cj.ro

[c]Prof. T. A. Jung, M. Heydari

Laboratory for X-ray Nanoscience and Technologies, Paul Scherrer Institut, 5232 Villigen, PSI, Switzerland

E-mail: thomas.jung@psi.ch

[d]Prof. M. Stöhr

Zernike Institute for Advanced Materials, University of Groningen, Nijenborgh 4, 9747 AG Groningen, The Netherlands, E-mail: m.a.stohr@rug.nl

[e]Dr. S. S. Zaman

Habib University, Block 18, Gulistan-e-Jauhar, University Avenue, Off Shahrah-e-Faisal Rd, Karachi-75290, Sindh, Pakistan, E-mail: sameena.shahzaman@sse.habib.edu.pk

[f]Prof. L. H. Gade

Anorganisch-Chemisches Institut, Universität Heidelberg, Im Neuenheimer Feld 270, 69120 Heidelberg, Germany, E-mail: lutz.gade@uni-hd.de

Abstract:

Host-guest architectures provide ideal systems to investigate site-specific physical and chemical effects. Condensation events in nanometer sized confinements are particularly interesting for the investigation of inter-molecular and molecule-surface interactions. They may be accompanied by conformational adjustments representing induced fit packing patterns. Here, we report that the symmetry of small clusters formed upon condensation, their registry with the substrate, their lateral packing as well as their adsorption height is characteristically modified by the packing of cycloalkanes in confinements. While cyclopentane and cycloheptane display cooperativity upon filling of the hosting pores, cyclooctane and to a lesser degree cyclohexane diffusively re-distribute to more favoured adsorption sites. The dynamic behaviour of cyclooctane is surprising at 5K given the cycloalkane melting point above 0°C. The site-specific modification of the interaction and behaviour of adsorbates in confinements plays a crucial role in many applications of 3D porous materials as gas storage agents or catalysts/bio-catalysts.

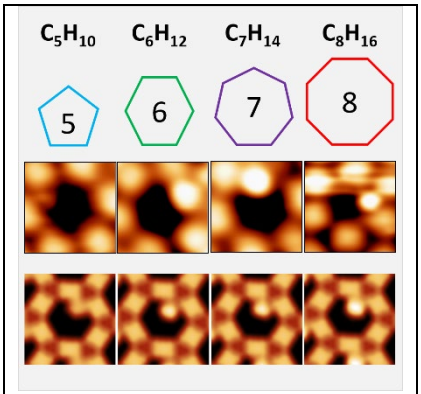

TOC Figure: Molecular condensation in nanometersized confinements: Site-specific nucleation and aggregation as well as other physico-chemical properties revealed by experiment and theory.

A large part of the present knowledge about the condensation of molecules has been derived from thermodynamic principles and from macroscopic or statistically averaged investigations of gases, fluids and large numbers of nucleates.[1–4] The wealth of more recent and increasingly conclusive experimental data provided an entry point to the microscopic understanding of inter-molecular forces governing the physical chemistry of matter[5,6]. In conjunction with theory and subsequent numerical modelling such understanding may allow for the prediction of structure property and structure activity relationships in materials science and chemistry as well as molecular life-sciences[7,8]. In particular growth studies at surfaces and interfaces,[9,10] on the atomic scale and within confinements[11] have accrued considerable insight into the site-specific mechanisms and contributed to the understanding of nucleation, the evolution of structural ordering[12,13] and the mechanisms of self-assembly[14–18]. Such insight into the physical forces, electronic states and the chemistry at different sites plays a key role in the prediction and control of bottom-up nanostructuring of functional surface materials[19–22].

Previous condensation studies predominantly covered homo-epitaxial or hetero-epitaxial systems with a small number of atomic components and simple structure, e.g. spherical or planar shape, on substrates with little or simple defects[23]. Conformationally flexible molecules, in contrast, may behave characteristically different due to the possibility to flex upon adsorption and upon compression inside confinements. As objects of study we have chosen a series of non-planar, conformationally flexible cyclo-alkanes (c-alkanes)[24] to study their site-specific condensation in the confinement provided by 1.6 nm sized pores in a surface supported coordination network[25].

Cycloalkanes represent a textbook model case for variable, size-dependent shape and conformational flexibility[26–30]. Their investigation inside confinements follows up on earlier experience gathered with porphyrins, C_{60}[31,32] and atomic Xe[33–38] nucleating at different specific sites of on-surface coordination networks[39,40]. The molecular structures of c-alkanes are determined by the tetrahedral angle between the sp^3 carbon bonds thus precluding planar configurations, as observed for aromatics. Different non-planar conformations allow for a characteristic temperature dependent dynamicity constrained by the ring-closing covalent bonds which affect the specific heat and the crystal packing[41].

The confinements used for the condensation experiments in this work are based on the highly stable Cu-coordinated network of triply dehydrogenated 4,9-diaminoperylene quinone-3,10-diimine (3deh-DPDI) generated by a thermal process on Cu(111)[39,42]. The porous surface network converts the free electrons in the 2D Shockley surface state of the underlying substrate into a specific spectrum of confined surface states (CSS). Each pore contains a partially localized electronic ground state giving rise to a peak in the electronic density of states (DOS) at 211 meV below the Fermi level (E_F) with both localized and non-localized components. In similarity to the earlier investigated Xe[33–38] cases, the interaction of the closed-shell c-alkanes with the pore containing a confined electronic state is governed by a combination of van der Waals forces and Pauli repulsion.

As will become apparent, the shape-adaptability of the c-alkanes not only adds an 'induced fit' element to their condensation within surface cavities, but also gives rise to collective rearrangements as exemplified by their interaction with the confined states within the pores of the surface network. Both intermolecular packing patterns and interaction with the site-specific electronic states give rise to filling-level dependent adsorption modes of the molecules in the pores. Using scanning tunnelling microscopy and spectroscopy (STM/STS) at low (5K) temperatures, we investigated the combined effects of the adaptive adsorbate structures and electronic forces on the site-specific condensation of 1 to 7 molecules. This is complemented by theoretical modelling based on density functional theory (DFT).

To compare the condensation of c-alkanes inside the confinements of a porous surface network and on bare Cu (111) (Figure 1) we exposed a considerable number of samples partially covered by the Cu-coordinated 3deh-DPDI network to four different c-alkanes, C_5H_{10} (**c5**), C_6H_{12} (**c6**), C_7H_{14} (**c7**) and C_8H_{16} (**c8**). Upon exposure to ~120 Langmuir a fraction of the pores was found to be partially / fully occupied, as revealed by STM. The pores at their maximal filling level accommodate seven c-alkane molecules in the case of **c5**, **c6**, **c7** but only four in the case of the larger **c8**. Figure 1 (3rd row) presents the arrangements of

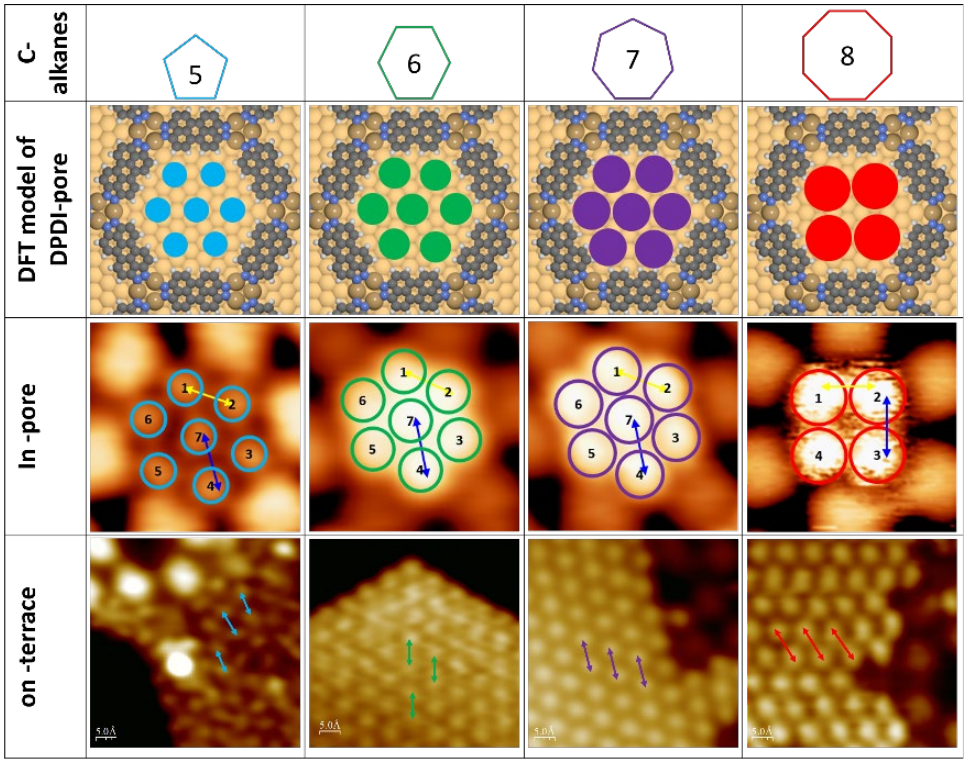

In pore	6.4	5.9	5.7	7.5
Terrace	6.4	6.3	7.2	8.1
D_t-D_p (%)	0 (0%)	0.4 (7%)	1.5 (21%)	0.6 (8%)

Figure. 1: Condensation of c-alkanes in confinements and on bare Cu(111). *Top two rows*: schematic chemical structure and condensation of c-alkanes in DPDI pores. The differently sized symbols within each row are drawn to scale in order to represent the increasing footprint from the smallest to the largest investigated c-alkane. *Third and fourth row*: STM images of pores at maximum observed occupancy and as 2D condensed islands on network free terraces. In the pores, the spatial confinement increases with increasing size of the c-alkanes as reflected by the decrease of the intermolecular distance. The four **c8** molecules in addition to their dynamicity, exhibit the largest intermolecular spacing. As a guide to the eye, coloured circles (blue-**c5**, green-**c6**, indigo-**c7**, red-**c8**) have been added to highlight the approximate position and size of the c-alkanes. *Table at the bottom*: c-alkanes except **c5** show an increased intermolecular spacing on network free areas. **c5** @ occ-7: ~0%, **c6** @ occ-7: ~7%, **c7** @ occ-7: ~21%, **c8** @ occ-4: ~8% compression by the confinement. D_t indicates the intermolecular distances within single layer islands on bare Cu(111) surfaces while D_p indicates the intermolecular distance inside pore. STM parameters: 2.4 nm x 2.4 nm, 1V, 6pm.

different c-alkane molecules at maximum pore occupancy. Only **c5** appears to be adsorbed with some space between the different molecules. At full occupancy (occ-7), six **c5** molecules adsorb in the corners in proximity to the network node, while the center molecule appears with a characteristic 'folded-edge' shape. Similarly, this filling pattern is repeated with little or no residual intermolecular space for **c6** and **c7**. The four **c8** molecules that can be observed at maximum occupancy of a pore, however, appear to be mobile at 5K and are assuming a rectangular (distorted square) arrangement which breaks the 3-fold symmetry of the underlying Cu(111) substrate and the geometry of the pore / confinement. In the table at the bottom of Figure 1, the inter-molecular distance of c-alkanes has been evaluated for each case. All c-alkanes except for **c5**, appear significantly 'compressed' at maximum occupancy in the pores compared to the 2D islands assembled on terraces of the bare copper surface. The intermolecular degree of lateral compression, as derived from the distances between the

geometric centers of the molecules is tabulated in the bottom row of the table in Figure 1. It was found to be insignificant in the case of **c5**, indicating lateral packing which is unperturbed by the confinement in a surface pore, but rises to ~7% for **c6** and to 21% for **c7**. The latter may be regarded as resulting from induced fit of **c6** and **c7** within the enclosures generated by the surface network. Even in the case of four molecules contained in the confining pore, the **c8** molecules appear compressed and with an inter-molecular distance reduced by ~8% in comparison to 2D islands on metal terraces.

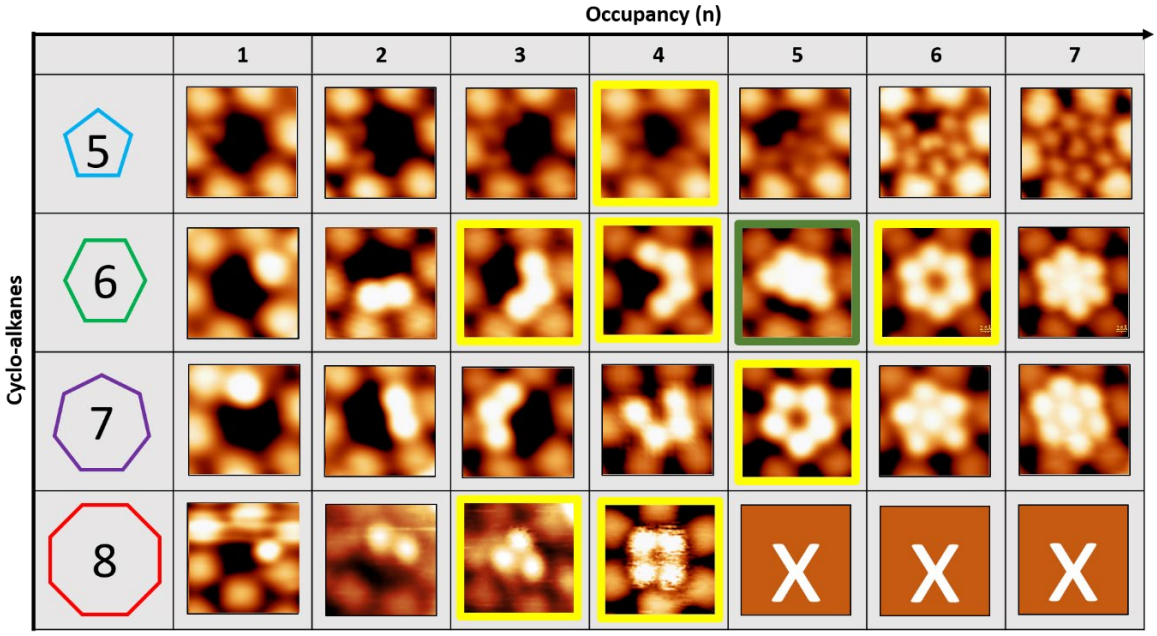

Figure 2: Molecule by molecule self-assembly of c-alkanes in confinements. STM images of pores filled with increasing numbers of c-alkane molecules are arranged with increasing occupancy (n) along the horizontal axis. The vertical axis labels the size of the c-alkane investigated. The number of different configurations observed in the pores has been indicated by a colour code: (yellow: two configurations, green: three configurations; the full dataset has been presented in Fig. SI-1). Interestingly in the case of **c8** a higher frequency mobility in the order of ~1/20th of the scan width (62 msec) becomes apparent. (STM parameters 1V, 6pA, image size 2.4 nm x 2.4 nm, pixels per frame: 256 px, scan speed 2nm/sec)

For further in-depth understanding of the c-alkane filling into the pores, we statistically analysed all possible occupancies up to maximum filling level (see Figure S1). The spontaneously occurring occupancies cover a full range from 0—7 molecules in case of **c5**, **c6**, **c7** and from 0—4 molecules with **c8**. In the following discussion, the occupancy of a pore with e.g. 3 molecules is denoted occ-3, and an overview of all filling configurations is displayed in Figure 2. Sometimes two (three) different configurations for a given occupancy have been observed as indicated by the yellow (green) frame around each image. The complete data set is shown in Figure S1. Similar to our earlier observations for Xe[35], c-alkanes at low occupancy, prefer to adsorb around the outer rim of the confinement. Consistently, this reflects the repulsive interaction of the molecules with the centrally located confined surface state (CSS) and, possibly, the weak van der Waals attraction experienced close to the network backbone.

The symmetry of the condensates relative to the apparent 6-fold symmetry of the pores (Note that the overall symmetry of the pores on the surface is reduced, only 3-fold due to the on-top and hollow registry of the corners of the network[25]) is interesting: While the pattern

formed by **c5** in the pores at all filling levels remains commensurate with the hexagonal pore, **c6** shows two five-fold symmetric arrangements among a total of three at occ-5. The next homologue, c-heptane **c7**, overrides the symmetry of the hosting site already at occ-3 and also assumes a pentagonal arrangement at occ-5 and occ-6 before resuming the 6-fold symmetry at full (occ-7) occupancy. Cyclooctane **c8** at occ-3 appears quite randomly adsorbed while the mobile square shaped arrangement at full occupancy (occ-4) clearly violates the hexagonal symmetry. Among all investigated cases, the only configuration with a visible mobility on the ~msec timescale accessible to STM analysis is **c8** at full occupancy (occ-4), whereas such mobility is not observed on the bare metal terraces where 2D islands predominate. A notable observation is the average time scale of the in-pore displacement in the order of ~60 msec for a molecule in presumably adsorbed state at 5K.

The situation of both the symmetry modification, the compression and the mobility of **c8**, is a plausible consequence of a weak interaction of the c-alkane with the substrate via multiple contact points. In comparison, Xe as an atom dominantly interacts with the substrate atoms underneath as reflected by its preferred on-top adsorption while shifting to non-registry sites under certain (lower packing density) conditions in this pore[35]. On the other hand, c-alkanes **c6** to **c8** but not **c5** flexibly respond by adaptations of symmetry and compression to accommodate a higher number of molecules in the available free area within the pore before they are 'elevated' into a new mode of condensation, at least for the center molecules of **c6** and **c7** and in the case of **c8** at occ-4 (Figure S2).

To obtain a homogeneous set of structures and properties, we employed DFT to re-calculate[43–46] the characteristic ground state and the most relevant excited state conformers of **c5**, **c6**, **c7** and **c8** (Table 1). The uneven C atom containing c-alkanes, in particular **c5**, remain closer to planar, with the latter having only one CH_2-group raised above the plane defined by the other four C atoms while the even c-alkanes can undergo conformational transitions at different activation energies.

In our DFT modelling, we have re-assessed the conformational states of all investigated c-alkanes and confirmed the well-known conformational ground states of the free molecule and the relative energy levels. Notably both, the energy difference between different states and the activation energies reported by others[27] reveal values for conformational transitions which are too high to be observed in our experiments performed at 5K corresponding to a thermal energy of only 0.5 meV. This includes the single conformer of **c5** which can convert from one envelope state to its neighbour with an estimated energy barrier of 0.5 kcal/mol (21 meV) corresponding to a temperature of ~250K[27]. It is however important to note that the molecule **c5** in its envelope conformation with 4 carbon atoms in the same plane can be stabilized more readily by surface-molecular interaction than the higher order c-alkanes. The results of DFT modelling confirm that **c5** adsorbs in 4-corner trapezoidal form with the 5th carbon atom forming a "flap" pointing towards the pore periphery while being randomly orientated for the central molecule in a full (occ-7) pore. We note, however, that the absence of conformational transitions at 5K does not preclude mobility of the molecules during their deposition on the 5-10K 'cold' sample before they are 'frozen' in certain molecular configurations.

DFT optimized molecule	C_5H_{10}	C_6H_{12}	C_7H_{14}	C_8H_{16}	
free	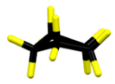 envelope	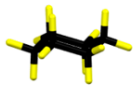 chair	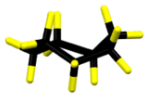 chair	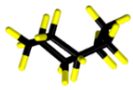 boat chair	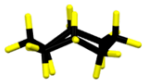 crown
$c\hat{t}c_{free}$	103.93	111.41 (109.5 ~ sp3 C)	115.11	116.49	117.73
ΔE_1		0.26 twist boat	0.13 boat	0.07 crown	
ΔE_2		0.50 boat		0.12 boat	
ΔE_3		0.62 half chair			
on-surface	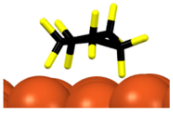 envelope	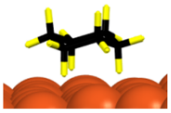 chair	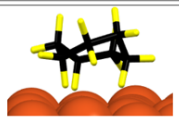 chair	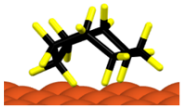 boat chair	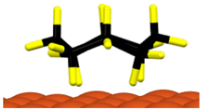 crown
$c\hat{t}c_{surface}$	105.25	112.20	116.36	116.98	118.82
in-pore	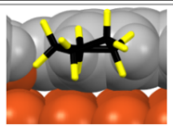 envelope	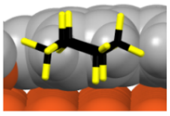 chair	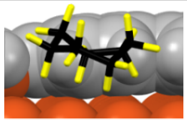 chair	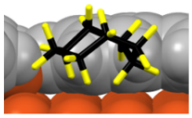 boat chair	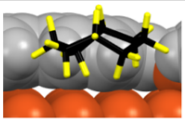 crown
$c\hat{t}c_{pore}$	105.07	111.88	115.82	117.04	117.41
$c\hat{t}c_{free}$ -$c\hat{t}c_{pore}$	1.14	0.47	0.71	0.55	-0.32
$\Delta E_{def_surface}$	0.05	0.06	0.05	0.07	0.09
ΔE_{def_pore}	0.04	0.05	0.06	0.05	0.06

Table 1: Summary of DFT calculations of the c-alkanes c5 to c8 in free space, on Cu(111) surface and inside the nanometer sized confinement. **"free"** (top 6 rows): In free space, depending on the size of the c-alkanes, different energy minimal and higher energy conformations have been identified in agreement to earlier reports and textbooks[27]. Beyond the shown ground state conformation, the higher energy conformers are listed by their structure category and energy difference, if applicable. The covalent ring causes the different energy minimal configurations to deviate in their bond angle $c\hat{t}c_{free}$ from the sp3 angle of 109.4 with **c6** getting closest to the tetraeder angle of the undistorted sp3 covalent bond. "**on-surface**" (center two rows) The intramolecular balance of forces is modified by relaxation of the molecule in the surface potential and characteristically different energy minimal structures arise as identified by the average bonding angle $c\hat{t}c_{surface}$. The 1.14 degree difference between the bond angle of the free and the in-pore adsorbed **c5** ($c\hat{t}c_{free}$ - $c\hat{t}c_{pore}$) reflects its larger planarization upon on-surface adsorption compared to the other three cases where the initially less planar structures are resisting. "**in-pore**" (bottom five rows). The modified surface potential in the confinement leads to the modification of energy minimal conformations and the corresponding average bond angles. The modified adsorption is also reflected by the deformation energies for on-surface and in-pore adsorption listed here (All Angles $c\hat{t}c$ are in degrees and energies ΔE are in eV).

Comparing the DFT calculated structures in free space with those modelled in on-surface (Figure S6) and in-pore configuration, reveals how the local surface potential affects the conformation, binding energies and average bonding angles. Notably, the least puckered **c5** shows a significantly stronger bonding angle deviation by adsorption than the other more 'three

dimensional' c-alkanes which enables the highest ratio, i.e. 4 out of 5 CH_2-units to maintain direct contact with the metal substrate.

For further analysis, we performed detailed measurements of the apparent STM height of the adsorbates at different occupancy levels in the pores and on terraces, with the DPDI network backbone as a reference. For all c-alkanes adsorbed in the pores, with the exception of **c5**, we found significantly increased apparent STM heights (**c6**: +0.24 Å, **c7**: +0.33 Å and most remarkably **c8**: +0.52 Å (~23 %) compared to 2D aggregate islands on the bare metal terraces (see second column in Table 2 and also in Figure S3). Notably, **c5** is found to be the only molecule appearing lower than the planar DPDI molecules in the surrounding network backbone. The apparent height evolution with increasing occupancy level is generally small for all molecules. For **c5** it is insignificant while there is a height increase for **c6** (<5%), **c7**(~2%) and **c8** (~2%) as full occupancy is reached. Notably, the predominant height increase occurred for the central 'key stone' molecule in the case of **c6** and to a lesser degree **c7** (Figure S3.1). The increased height, in particular that of the centrally located molecule is characteristic for a modified adsorption. The 'misfit' of the central molecule can be attributed to the increased readjusted (induced fit) 2D packing density and therefore intermolecular repulsion and, possibly, also to the expected maximum Pauli repulsion with the confined surface state in the center of the pore. The less puckered conformation of **c5,** on the one hand, and the non-availability of a planar conformation for **c6** to **c8** on the other, appears to be the cause for the site dependent contrast change. Notable is the lateral 'on-the-spot' motion for **c8** in the full pore, a behaviour which is unexpected for molecules adsorbed on a metal held at 5K.

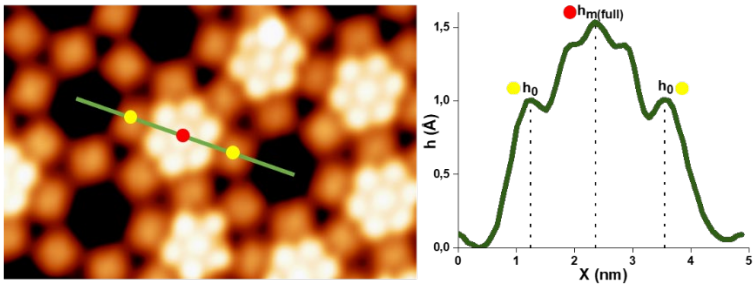

C-alkanes	$(h_{m(full)}-h_t)^{EXP}$	$(h_{m(1)}-h_0)^{EXP}$	$(h_{m(full)}-h_0)^{EXP}$	$(h_m-h_0)^{LDOS}$
C_5H_{10}	0.01	-0.28	-0.29	-0.22
C_6H_{12}	0.24	0.34	0.49	0.31
C_7H_{14}	0.33	0.45	0.53	0.40
C_8H_{16}	0.52	0.58	0.62	0.63

Table 2: Tunnelling apparent height analysis of the c-alkanes: $\mathbf{h_{m(i)}}$ denominates the molecular height $\mathbf{h_m}$ measured within a **i**-fold populated pore, $\mathbf{h_t}$ is molecular height on terrace and $\mathbf{h_0}$ is DPDI height. -From left to right $\mathbf{(h_{m(full)}-h_t)^{EXP}}$ This column lists the apparent height difference of the molecules within supramolecular islands on network-free terrace areas and in the fully occupied pore. **c5** is the only molecule not showing a significant apparent height increase by its in-pore adsorption. $\mathbf{(h_{m(1)}-h_0)^{EXP}}$, $\mathbf{(h_{m(full)}-h_0)^{EXP}}$ These two columns compare the apparent height increase for the molecules adsorbed in the pore at single occupancy and the center

molecule at full occupancy. Again **c5** takes a special role (negative values, i.e. lower apparent height than DPDI, absence of significant height increase and presumably filling level and location-independent adsorption). **c6** and **c7** show the most significant height increase as it is plausible from their higher in-pore compression compared to **c8** as discussed in Figure 1. In the last column $\mathbf{(h_m\text{-}h_0)}^{\mathbf{LDOS}}$, the DFT calculated height differences (LDOS) have been tabulated. The values are in good agreement with the experimental data in the neighbouring column and establish the numerical modelling to be appropriate. All values are given in Å.

The relative energetics of different condensation states may be analysed by looking at the frequency of their occurrence after deposition at 5K. The histogram of pore occupancy (Figure 3) reveals no significant peak among the partially occupied pores, indicating that there are no 'magic' filling levels / clusters[35]. Notably, full (occ-7) pores of **c5** & **c7** are strikingly frequent in comparison to their lower occupancy condensates (occ-0 – occ-6). Only a small fraction of the counted pores is partially filled (~1/8th for **c5** and 1/10th for **c7**). This indicates that pores keep filling up by capturing molecules during the deposition process until they are fully occupied. The histogram of **c6** & **c8** is distinctively different in that full occupancy and all partial occupancies are about equally probable. For **c8** this phenomenon is accompanied by an exceptionally high fraction of empty pores and also a very high fraction of molecules condensed in close packed islands on the network-free terrace area.

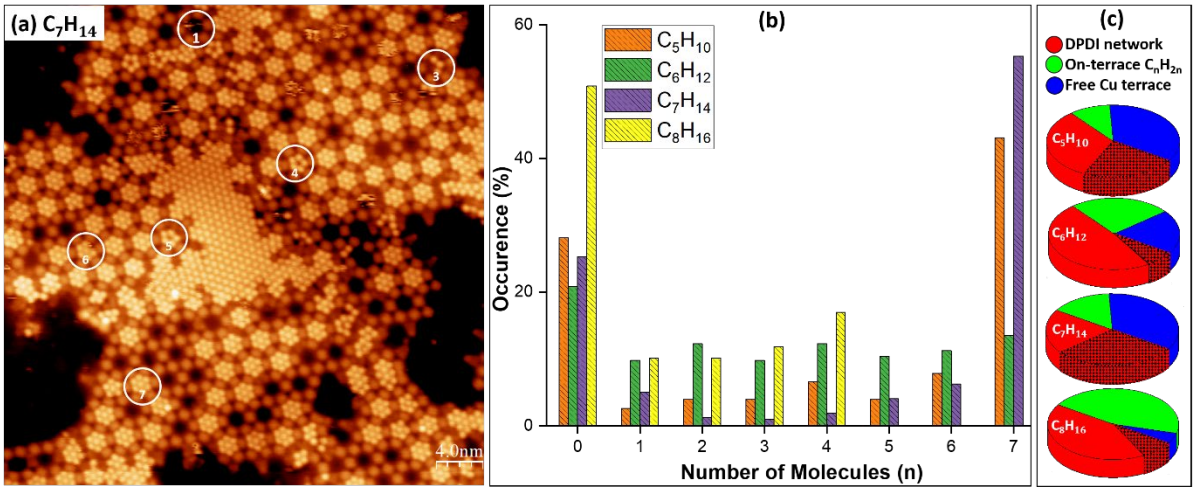

Figure 3: Condensation statistics of the c-alkanes adsorbed in-pore and on-terrace sites. (a) STM overview of **c7** adsorbed in DPDI pores and also on the bare metal terrace. **(b)** Histogram analysis showing the statistical distribution of different molecules in pores of different occupancy (n). Analysis performed after 120L exposure. The condensation of the c-alkanes follows two different schemes for the uneven C atom containing c-alkanes, for **c5** and **c7** the condensation histogram is dominated by 7-fold clusters i.e. by fully filled pores. Thus, partially filled pores exhibit a high propensity to capture adsorbates until they are completely full and cannot adsorb more. The rate-limiting step is comprised by the initial condensation of the first c-alkane in an empty pore. **c6** and **c8**, in contrast exhibit a rather homogeneous occupancy distribution: The differently populated pores exhibit a more equal probability to capture another c-alkane. **(c)** Pie charts indicating the relative c-alkane coverage in the different surface compartments. (red) Network covered area: The dotted sector at the bottom right corresponds to the fraction of the surface area with fully filled pores among the available network coverage; (green) the four different c-alkanes occupy a considerably different fraction of the network free metal (blue) in spite of the similar DPDI network coverage. **c5** and **c7** show a considerable affinity to fill network pores, **c6** and even more **c8** prefer to expand 2D islands on the bare metal. This non-linear filling statistics evidences their different affinity to nucleate and progressively fill the pores (cf. For more details see Figure S2). The network coverage of all four samples is ~50%;

While **c5** and **c7** clearly show a trend towards full, i.e., 7-fold occupancy, the two even numbered c-alkanes **c6** and in particular **c8** exhibit different statistics. Here, all partial occupancies as well as full occupancy are about equally frequent. Furthermore, we note that already at very low exposures for **c8** only a very small fraction of molecules is entering the pores compared to their accumulation in 2D islands on the metal terraces. The rather high gas-phase heat capacity of **c8** at 300K (thermodynamic state of the molecule during the exposure and adsorption) (147.19 J/molK * K)[41] together with its significant flexibility, translates into higher entropic motion, and may be the cause of the low sticking coefficient of this molecule in the pores (Figure S2).

Confined surface states (CSS) within confinements generated on surfaces of coinage metal substrates[33,39] interact with guest molecules and may thus act as probes for their adsorption. Scanning tunneling spectroscopy (STS) measurements performed above the voids of the surface network revealed the shift of the CSS to energies closer to E_F compared to the empty pore level (211 mV below E_F). Such quantum mechanical confinement in out-of-plane direction can be imposed by any adsorbate[33]. The shifted position of the CSS which results from the deposition of guest molecules is due to Pauli repulsion between the molecular orbitals and substrate states and is measured for the different c-alkanes at varying occupancies (Figure 4). It is found that an occupancy of four molecules of **c6** induced an upshift to 67 meV below E_F (see table in Figure 4) which is significantly more pronounced than the CSS shift observed for such pores fully filled with 12Xe atoms for which the shift remains at a level 147 meV[33] below E_F. In marked contrast to the monotonic up-shifting reported for successive Xe condensation[33], the CSS shifts observed for various occupancies of cycloalkanes reverts back towards reduced interaction with further increased occupancy, i.e. the CSS moves closer to the position corresponding to the empty pore upon approaching full occupancy. In particular, the final step towards the full pore by insertion of the 'keystone' molecule is clearly associated with a strong back shift towards lower Pauli repulsion. We have also observed that odd-numbered c-alkanes **c5** and **c7**, preferably condense in pores at increased occupancy (vide supra). For these, the repulsive interaction with the CSS appears to be ~30 meV lower than observed for **c6** and **c8** with their preferred condensation on the network-free terraces (Figure S5).

This specific non-linear behavior of the strong CSS energy shift, first towards E_f and then reverse upon increased pore occupancy observed for **c6** (Figure 4b) is observed for all investigated c-alkanes and has to be related to a phenomenon not occurring with Xe[33]. The CSS is progressively confined (in space) and therefore shifted (in energy / position with reference to E_f) by two effects: By lateral confinement with the i) shrinking adsorbate-free surface area in the pore and by out-of-plane confinement with the ii) modified balance of Pauli repulsion and London forces (also referred to as pillow effect[47]) compressing the surface state. This out-of-plane confinement is common to c-alkanes and the previously studied Xe alike, but, at first sight, fails to explain the reverse shifting of the CSS in the direction of a reduced interaction (vide infra).

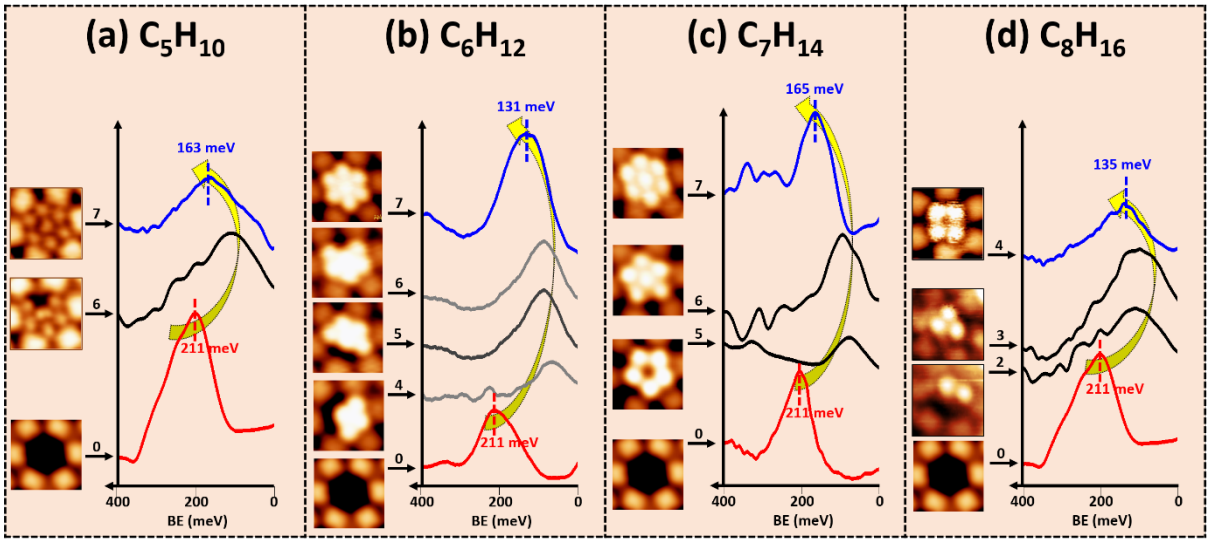

C-alkanes	0	2	3	4	5	6	7
C_5H_{10}	211 meV	---	---	---	---	109 meV	163 meV
C_6H_{12}	211 meV	---	---	67 meV	85 meV	95 meV	131 meV
C_7H_{14}	211 meV	---	---	----	76 meV	92 meV	165 meV
C_8H_{16}	211 meV	109 meV	116 meV	135 meV	XXX	XXX	XXX

Figure 4: Different numbers of c-alkanes inside pores and their influence on the CSS below the pore. dI/dV spectra have been acquired at the center of the vacancy island of each pore, or in the pore center for full pores. **(a)-(d)** The spectra are displayed together with the corresponding STM images (2.5nm X 2.5nm) acquired for pores hosting different numbers of **c5**, **c6**, **c7** and **c8** molecules respectively, as indicated. With initially increasing occupancy the Pauli repulsion between the molecules and the underlying CSS induces a shift towards higher BEs (i.e. towards the Fermi Energy E_F). There is a remarkable non-linearity in the position of the CSS: It shifts back towards the empty pore BE above a certain filling level. The shifting CSS peak positions have been tabulated for the different c-alkanes and pore populations below. Note the most significant back-shift occurring above occ-4 for **c5** to **c7** and above occ-2 for **c8** respectively. The data sets are not equally dense for all c-alkanes because the acquisition had been obstructed in some cases (e.g. **c5**, generally more at lower occupancy) by the molecules being picked up by the tip during the acquisition of the I/V spectra).

Before discussing the pronounced non-linear behavior of the CSS energy at variable occupancies, its generally greater response to c-alkanes compared to Xe needs to be addressed. The physisorption of both, Xe atoms[34] and c-alkanes in the pore is dominated by London dispersion forces and Pauli repulsion, with the former being crucially determined by the polarizability of the adsorbate and the adsorbent. The polarizability of c-alkanes filling a pore[48] is up to three times higher than that of Xe at full, 12-fold filling. The London force and physisorption strength of the deposited c-alkanes are thus expected to be stronger compared to Xe, which is consistent with the observed, pronounced shift of the CSS at low c-alkane occupancies. Occupancy with c-alkane **c6** (**c7**) for example gives rise to a maximum shift to only 67 meV (76 meV) below E_F at occ-4 (occ-5) and maximum back-shift 131 meV (165 meV) at full occ-7 (Figure 4. and the table below). Notably, the energy position of the CSS at full c-alkane occupancy is back to a range similar to the fully Xe occupied reference (147 meV below E_F). This back-shift is slightly higher for **c5** and **c7** (~164meV), and slightly lower for **c6** and **c8** (~132 meV below E_F).

The observed energetic reverse-shift of the CSS upon approaching full occupancy of the pores is in contrast to the monotonic evolution previously observed for Xe atoms and attributed to the different adsorption behavior of the c-alkanes compared to Xe. Xe atoms adsorb in on-top sites on the metal substrates, and predominantly adsorb in the root(3) x root(3) rot 30 superstructure. Even at full 12-fold occupancy no compression is observed for Xe in pores. Upon increased 2D packing of **c6** to **c8**, however, the in-pore arrangement which is formed violates the symmetry of the substrate underneath and relates to the lateral compression, STM height changes and mobility mentioned above. Cycloalkanes, possess non-planar structures with a large number of conformational degrees of freedom, whereas for Xe atoms and likewise for planar or close to planar porphyrin derivatives[49] and the like[50], there are no (few) internal degrees of freedom affecting the adsorption state. As a consequence, the CH2 units of the c-alkanes interact unequally with the substrate and changes in the surface potential are expected to lead to a re-equilibration of the molecular conformation as listed in Table 1. DFT modelling has shown (Figure S7) that for the c-alkanes in the gas phase all bonds are of equal length, giving rise to the most relaxed structure, while being most perturbed (and distorted) in contact with a bare metal surface. This trend is also reflected in the distortion of the bond angles ($\angle ccc_{free}$ - $\angle ccc_{pore}$ in Table 1) The modified ground-state conformation and the resulting packing pattern of the molecules affects the dispersive interaction and Pauli repulsion with the CSS within the pores and is further enhanced by the sterically required lateral compression for the larger c-alkanes **c6** to **c8** at full occupancy. As additional evidence for the re-equilibration of the guest molecule clusters in the confinements upon complete filling, we refer to the elevated center molecule (**c6** and **c7**) (Table 2) and, implicitly, to the dynamicity of fully occupied (occ-4) c8. Both phenomena indicate that the observed non-linear behaviour is caused by the modified collective balance between London dispersion forces and Pauli repulsion. Particularly noteworthy are the substantial changes for the c-alkanes differing only by one C unit. The latter appear to be significantly affecting the adsorption energetics as well as the sticking coefficient. These observations raise questions about the role of these factors in the non-equilibrium dynamics of nucleation and condensation.

Our analysis of the condensation of c-alkanes (**c5** – **c8**) within the pores of an on-surface network reveals an unprecedented complexity which at first glance is unexpected for a small molecule adsorbing in nanometer sized and atomically precise confinements. We find that the c-alkanes change their adsorption mode, as reflected by their compression, their symmetry violation with regard to the hosting pores and by their non-linear interaction with the confined surface state (CSS). With increased 2D packing/compression, the c-alkanes adapt their conformation and the interaction forces with the confining walls and the Pauli repulsion with the underlying CSS. This is in stark contrast to Xe atoms behaving like hard spheres in a bowl in absence of conformational degrees of freedom. The former, c-alkane can change its conformation and adsorption state, while the latter, Xe, is 'hard' due to the closed shell electronic shell structure of the noble gas Xe. It is generally expected, also for differently sized pores, that the competition between available in-pore surface area and the 'footprint' of the adsorption determines the highest number of adsorbates. In the case of four **c8** molecules in one pore, the site specific / environment specific enthalpy / entropy balance is so strongly modified that molecular dynamicity becomes visible at 5K. This mobility is unexpected at 5K

and in stark contrast to the melting point of solid **c8** crystals at 288K. The complexity of c-alkane condensation in the confinements motivates further temperature dependent investigations combined with theoretical modelling of other molecules with some conformational degree of freedom in different sized networks[51] to provide a better understanding of the complex entropy / enthalpy balance governing this phenomenon.

In this work, we provide first real-space evidence for the general phenomenon of the conformational response of complex molecules upon their confinement within cavities defined with atomic precision. The internal reorientation of guest molecules is reminiscent of the induced fit concept invoked for enzyme/substrate interactions and is expected to be a general phenomenon for such inclusion processes, both on surfaces and in porous solids. The ability to address these individually and to investigate local properties in a one-by-one fashion is a new opportunity. It may facilitate the rationally driven development of functional materials, inter-alia catalysts, in which such molecule-host interactions at interfaces play a crucial role.

ASSOCIATED CONTENT

Supporting information is available free of charge at [link to be provided by Editorial Office]. This includes a more elaborate and referenced description of the methods used and of the experimental set-up. Also complete sets of Scanning Microsocopy and Spectroscopy data is included there, together with cross-sectional and statistical analyses in histogram form or as tables. Also, SI includes more elaborate numerical simulation data and analyses, all as referenced in the main text.

AUTHOR CONTRBUTIONS:

Corresponding authors:

Aisha Ahsan- Department of Physics, University of Basel, Klingelbergstrasse 82, 4056 Basel, Switzerland, E-mail: aisha.ahsan@unibas.ch

Thomas A Jung- Laboratory for Micro- and Nanotechnology, Paul Scherrer Institut, 5232 Villigen, PSI, Switzerland, E-mail: thomas.jung@psi.ch

Lutz H Gade- Anorganisch-Chemisches Institut, Universität Heidelberg, Im Neuenheimer Feld 270, 69120 Heidelberg, Germany, E-mail: lutz.gade@uni-hd.de

Authors:

A.A., in close collaboration with L.H.G and T.A.J. conceived the presented research. A.A. developed the sample preparation and characterization protocol, with input provided by T.N. S.N., R.Sk., S.F.M. and T.A.J. A.A. also performed the vast majority of the STM/S experiments, with the assistance of T.N. S.N., R.Sk., S.F.M., M.H. All these authors discussed the final analysis of the STM/S data together with S.S.Z, L.H.G and T.A.J., J.B. developed and provided the ab-initio DFT calculations of the on-surface molecular network and their electronic characteristics. L.B-I. and C.M. developed and provided simulations of the c-alkane molecules and their site-dependent assemblies and performed the analysis of the same. M.S. critically reviewed the exhaustive data on the on-surface molecular network. A.A., S.S.Z., L.B-I., C.M., L.H.G., and T.A.J prepared the figures and developed the layout

of the manuscript. A.A. wrote the original draft sections of the experimental, L.B-J. of the theoretical parts of the manuscript. All authors contributed to the final proofing of the data and the writing of the manuscript.

ACKNOWLEDGEMENTS:

M. Martina and R. Schelldorfer have provided crucial support towards the development of the experimental apparatus and the procedures. J. Björk is acknowledged for his decisive contribution to the understanding of the confined surface state and network by DFT simulations and for interesting and helpful discussion on the present manuscript. O. Popova had been participating in discussions on the earlier experimental data.

This research was co-funded by the Swiss National Science Foundation (grant no. 200020-149713, 206021-121461, 206021-113149, 206021-144991, and 200020-153549) and the National Centre of Competence in Research "Nanoscience" (NCCR-Nano, project "Nanoscale Science"), Swiss Nanoscience Institute (SNI) (project nos. P1204 and P1203), Commission for Technology and Innovation (CTI) contract no. 16464.1 PFNM-NM, University of Basel. L B.-I. and C. M acknowledged partial support from UEFISCDI Romania through PN-III-P4-ID-PCE-2020-0824 project. M.S. acknowledges funding from the Netherlands Organization for Scientific Research (NWO) (Vici grant 680.47.633).

REFERENCES:

(1) Molecules *. *Nature* **1873**, *8* (204), 437–441.
(2) Klein, M. J. The Historical Origins of the Van Der Waals Equation. *Physica* **1974**, *73* (1), 28–47.
(3) Yalkowsky, S. H.; Alantary, D. Estimation of Melting Points of Organics. *J. Pharm. Sci.* **2018**, *107* (5), 1211–1227.
(4) Yang, H.; Goudeli, E.; Hogan, C. J. Condensation and Dissociation Rates for Gas Phase Metal Clusters from Molecular Dynamics Trajectory Calculations. *J. Chem. Phys.* **2018**, *148* (16), 164304.
(5) Israelachvili, J. N. *Intermolecular and Surface Forces: Revised Third Edition.*; Elsevier Science: Burlington, 2011.
(6) Liptrot, D. J.; Power, P. P. London Dispersion Forces in Sterically Crowded Inorganic and Organometallic Molecules. *Nat. Rev. Chem.* **2017**, *1* (1), 0004.
(7) *HANDBOOK OF NANOPHYSICS: Clusters and Fullerenes.*; CRC PRESS: S.l., 2017.
(8) Atkins, P.; de Paula, J.; Keeler, J. *Atkins' Physical Chemistry*, 12th ed.; Oxford University Press: New York, 2022.
(9) Teyssandier, J.; Feyter, S. D.; Mali, K. S. Host–Guest Chemistry in Two-Dimensional Supramolecular Networks. *Chem. Commun.* **2016**, *52* (77), 11465–11487.
(10) Tang, J.-H.; Li, Y.; Wu, Q.; Wang, Z.; Hou, S.; Tang, K.; Sun, Y.; Wang, H.; Wang, H.; Lu, C.; Wang, X.; Li, X.; Wang, D.; Yao, J.; Lambert, C. J.; Tao, N.; Zhong, Y.-W.; Stang, P. J. Single-Molecule Level Control of Host-Guest Interactions in Metallocycle-C60 Complexes. *Nat. Commun.* **2019**, *10* (1), 4599.
(11) Maeda, N.; Israelachvili, J. N. Nanoscale Mechanisms of Evaporation, Condensation and Nucleation in Confined Geometries. *J. Phys. Chem. B* **2002**, *106* (14), 3534–3537.
(12) Zhou, Z.; Wei, Z.; Schaub, T. A.; Jasti, R.; Petrukhina, M. A. Structural Deformation and Host–Guest Properties of Doubly-Reduced Cycloparaphenylenes, [*n*]CPPs $^{2-}$ (*n* = 6, 8, 10, and 12). *Chem. Sci.* **2020**, *11* (35), 9395–9401.

(13) Rizzuto, F. J.; von Krbek, L. K. S.; Nitschke, J. R. Strategies for Binding Multiple Guests in Metal–Organic Cages. *Nat. Rev. Chem.* **2019**, *3* (4), 204–222.
(14) Qu, D.-H.; Wang, Q.-C.; Zhang, Q.-W.; Ma, X.; Tian, H. Photoresponsive Host–Guest Functional Systems. *Chem. Rev.* **2015**, *115* (15), 7543–7588.
(15) Furukawa, H.; Cordova, K. E.; O'Keeffe, M.; Yaghi, O. M. The Chemistry and Applications of Metal-Organic Frameworks. *Science* **2013**, *341* (6149), 1230444.
(16) Hendriks, F. C.; Valencia, D.; Bruijnincx, P. C. A.; Weckhuysen, B. M. Zeolite Molecular Accessibility and Host–Guest Interactions Studied by Adsorption of Organic Probes of Tunable Size. *Phys. Chem. Chem. Phys.* **2017**, *19* (3), 1857–1867.
(17) Kuhne, D.; Klappenberger, F.; Krenner, W.; Klyatskaya, S.; Ruben, M.; Barth, J. V. Rotational and Constitutional Dynamics of Caged Supramolecules. *Proc. Natl. Acad. Sci.* **2010**, *107* (50), 21332–21336.
(18) Wahl, M.; Stöhr, M.; Spillmann, H.; Jung, T. A.; Gade, L. H. Rotation–Libration in a Hierarchic Supramolecular Rotor–Stator System: Arrhenius Activation and Retardation by Local Interaction. *Chem Commun* **2007**, No. 13, 1349–1351.
(19) Yang, H.; Yuan, B.; Zhang, X.; Scherman, O. A. Supramolecular Chemistry at Interfaces: Host–Guest Interactions for Fabricating Multifunctional Biointerfaces. *Acc. Chem. Res.* **2014**, *47* (7), 2106–2115.
(20) Wankar, J.; Kotla, N. G.; Gera, S.; Rasala, S.; Pandit, A.; Rochev, Y. A. Recent Advances in Host–Guest Self-Assembled Cyclodextrin Carriers: Implications for Responsive Drug Delivery and Biomedical Engineering. *Adv. Funct. Mater.* **2020**, *30* (44), 1909049.
(21) Martin, P. M. *Handbook of Deposition Technologies for Films and Coatings Science, Applications and Technology*; Elsevier / WA: Amsterdam; Boston, 2010.
(22) Spillmann, H.; Kiebele, A.; Stöhr, M.; Jung, T. A.; Bonifazi, D.; Cheng, F.; Diederich, F. A Two-Dimensional Porphyrin-Based Porous Network Featuring Communicating Cavities for the Templated Complexation of Fullerenes. *Adv. Mater.* **2006**, *18* (3), 275–279.
(23) Müller, K.; Enache, M.; Stöhr, M. Confinement Properties of 2D Porous Molecular Networks on Metal Surfaces. *J. Phys. Condens. Matter* **2016**, *28* (15), 153003.
(24) *The Chemistry of Alkanes and Cycloalkanes*; Patai, S., Rappoport, Z., Eds.; The Chemistry of functional groups; Wiley: Chichester ; New York, 1992.
(25) Matena, M.; Björk, J.; Wahl, M.; Lee, T.-L.; Zegenhagen, J.; Gade, L. H.; Jung, T. A.; Persson, M.; Stöhr, M. On-Surface Synthesis of a Two-Dimensional Porous Coordination Network: Unraveling Adsorbate Interactions. *Phys. Rev. B* **2014**, *90* (12), 125408.
(26) Bocian, D. F.; Pickett, H. M.; Rounds, T. C.; Strauss, H. L. Conformations of Cycloheptane. *J. Am. Chem. Soc.* **1975**, *97* (4), 687–695.
(27) Dragojlovic, V. Conformational Analysis of Cycloalkanes. *ChemTexts* **2015**, *1* (3), 14.
(28) Pakes, P. W.; Rounds, T. C.; Strauss, H. L. Conformations of Cyclooctane and Some Related Oxocanes. *J. Phys. Chem.* **1981**, *85* (17), 2469–2475.
(29) Anet, F. A. L.; Krane, J. The Conformations of Cyclononane Dynamic Nuclear Magnetic Resonance and Force-Field Calculations. *Isr. J. Chem.* **1980**, *20* (1–2), 72–83.
(30) Hendrickson, J. B. Molecular Geometry. V. Evaluation of Functions and Conformations of Medium Rings. *J. Am. Chem. Soc.* **1967**, *89* (26), 7036–7043.
(31) Samuely, T.; Liu, S.-X.; Haas, M.; Decurtins, S.; Jung, T. A.; Stöhr, M. Self-Assembly of Individually Addressable Complexes of C_{60} and Phthalocyanines on a Metal Surface: Structural and Electronic Investigations. *J. Phys. Chem. C* **2009**, *113* (45), 19373–19375.
(32) Kiebele, A.; Bonifazi, D.; Cheng, F.; Stöhr, M.; Diederich, F.; Jung, T.; Spillmann, H. Adsorption and Dynamics of Long-Range Interacting Fullerenes in a Flexible, Two-Dimensional, Nanoporous Porphyrin Network. *ChemPhysChem* **2006**, *7* (7), 1462–1470.
(33) Nowakowska, S.; Wäckerlin, A.; Piquero-Zulaica, I.; Nowakowski, J.; Kawai, S.; Wäckerlin, C.; Matena, M.; Nijs, T.; Fatayer, S.; Popova, O.; Ahsan, A.; Mousavi, S. F.; Ivas, T.; Meyer, E.; Stöhr,

M.; Ortega, J. E.; Björk, J.; Gade, L. H.; Lobo-Checa, J.; Jung, T. A. Configuring Electronic States in an Atomically Precise Array of Quantum Boxes. *Small* **2016**, *12* (28), 3757–3763.

(34) Kawai, S.; Foster, A. S.; Björkman, T.; Nowakowska, S.; Björk, J.; Canova, F. F.; Gade, L. H.; Jung, T. A.; Meyer, E. Van Der Waals Interactions and the Limits of Isolated Atom Models at Interfaces. *Nat. Commun.* **2016**, *7* (1), 11559.

(35) Nowakowska, S.; Wäckerlin, A.; Kawai, S.; Ivas, T.; Nowakowski, J.; Fatayer, S.; Wäckerlin, C.; Nijs, T.; Meyer, E.; Björk, J.; Stöhr, M.; Gade, L. H.; Jung, T. A. Interplay of Weak Interactions in the Atom-by-Atom Condensation of Xenon within Quantum Boxes. *Nat. Commun.* **2015**, *6* (1), 6071.

(36) Nowakowska, S.; Mazzola, F.; Alberti, M. N.; Song, F.; Voigt, T.; Nowakowski, J.; Wäckerlin, A.; Wäckerlin, C.; Wiss, J.; Schweizer, W. B.; Broszio, M.; Polley, C.; Leandersson, M.; Fatayer, S.; Ivas, T.; Baljozovic, M.; Mousavi, S. F.; Ahsan, A.; Nijs, T.; Popova, O.; Zhang, J.; Muntwiler, M.; Thilgen, C.; Stöhr, M.; Pasti, I. A.; Skorodumova, N. V.; Diederich, F.; Wells, J.; Jung, T. A. Adsorbate-Induced Modification of the Confining Barriers in a Quantum Box Array. *ACS Nano* **2018**, *12* (1), 768–778.

(37) Ahsan, A.; Mousavi, S. F.; Nijs, T.; Nowakowska, S.; Popova, O.; Wäckerlin, A.; Björk, J.; Gade, L. H.; Jung, T. A. Phase Transitions in Confinements: Controlling Solid to Fluid Transitions of Xenon Atoms in an On-Surface Network. *Small* **2018**, 1803169.

(38) Ahsan, A.; Fatemeh Mousavi, S.; Nijs, T.; Nowakowska, S.; Popova, O.; Wäckerlin, A.; Björk, J.; Gade, L. H.; Jung, T. A. Watching Nanostructure Growth: Kinetically Controlled Diffusion and Condensation of Xe in a Surface Metal Organic Network. *Nanoscale* **2019**, *11* (11), 4895–4903.

(39) Lobo-Checa, J.; Matena, M.; Muller, K.; Dil, J. H.; Meier, F.; Gade, L. H.; Jung, T. A.; Stohr, M. Band Formation from Coupled Quantum Dots Formed by a Nanoporous Network on a Copper Surface. *Science* **2009**, *325* (5938), 300–303.

(40) Shchyrba, A.; Wäckerlin, C.; Nowakowski, J.; Nowakowska, S.; Björk, J.; Fatayer, S.; Girovsky, J.; Nijs, T.; Martens, S. C.; Kleibert, A.; Stöhr, M.; Ballav, N.; Jung, T. A.; Gade, L. H. Controlling the Dimensionality of On-Surface Coordination Polymers via Endo- or Exoligation. *J. Am. Chem. Soc.* **2014**, *136* (26), 9355–9363.

(41) Dorofeeva, O. V.; Gurvich, L. V.; Jorish, V. S. Thermodynamic Properties of Twenty-One Monocyclic Hydrocarbons. *J. Phys. Chem. Ref. Data* **1986**, *15* (2), 437–464.

(42) Stöhr, M.; Wahl, M.; Galka, C. H.; Riehm, T.; Jung, T. A.; Gade, L. H. Controlling Molecular Assembly in Two Dimensions: The Concentration Dependence of Thermally Induced 2D Aggregation of Molecules on a Metal Surface. *Angew. Chem. Int. Ed.* **2005**, *44* (45), 7394–7398.

(43) Ocola, E. J.; Bauman, L. E.; Laane, J. Vibrational Spectra and Structure of Cyclopentane and Its Isotopomers. *J. Phys. Chem. A* **2011**, *115* (24), 6531–6542.

(44) Tekautz, G.; Binter, A.; Hassler, K.; Flock, M. Chair, Boat and Twist Conformation of Dodecamethylcyclohexasilane and Undecamethylcyclohexasilane: A Combined DFT and Raman Spectroscopic Study. *ChemPhysChem* **2006**, *7* (2), 421–429.

(45) Freeman, F.; Hwang, J. H.; Hae Junge, E.; Dinesh Parmar, P.; Renz, Z.; Trinh, J. Conformational Analysis of Cycloheptane, Oxacycloheptane, 1,2-Dioxacycloheptane, 1,3-Dioxacycloheptane, and 1,4-Dioxacycloheptane: Conformational Analysis of Oxacycloheptanes. *Int. J. Quantum Chem.* **2008**, *108* (2), 339–350.

(46) Rocha, W. R.; Pliego, J. R.; Resende, S. M.; Dos Santos, H. F.; De Oliveira, M. A.; De Almeida, W. B. Ab Initio Conformational Analysis of Cyclooctane Molecule. *J. Comput. Chem.* **1998**, *19* (5), 524–534.

(47) Vázquez, H.; Dappe, Y. J.; Ortega, J.; Flores, F. Energy Level Alignment at Metal/Organic Semiconductor Interfaces: “Pillow” Effect, Induced Density of Interface States, and Charge Neutrality Level. *J. Chem. Phys.* **2007**, *126* (14), 144703.

(48) Filipe, E. J. M.; Dias, L. M. B.; Calado, J. C. G.; McCabe, C.; Jackson, G. Is Xenon an “Ennobled” Alkane? *Phys Chem Chem Phys* **2002**, *4* (9), 1618–1621.

(49) Wahl, M.; Stöhr, M.; Spillmann, H.; Jung, T. A.; Gade, L. H. Rotation–Libration in a Hierarchic Supramolecular Rotor–Stator System: Arrhenius Activation and Retardation by Local Interaction. *Chem Commun* **2007**, No. 13, 1349–1351.

(50) Stöhr, M.; Wahl, M.; Spillmann, H.; Gade, L. H.; Jung, T. A. Lateral Manipulation for the Positioning of Molecular Guests within the Confinements of a Highly Stable Self-Assembled Organic Surface Network. *Small* **2007**, *3* (8), 1336–1340.

(51) Shchyrba, A.; Martens, S. C.; Wäckerlin, C.; Matena, M.; Ivas, T.; Wadepohl, H.; Stöhr, M.; Jung, T. A.; Gade, L. H. Covalent Assembly of a Two-Dimensional Molecular “Sponge” on a Cu(111) Surface: Confined Electronic Surface States in Open and Closed Pores. *Chem Commun* **2014**, *50* (57), 7628–7631.